Flow past a flat plate at low Reynolds numbers

By E. JANSSEN
General Electric Company, San Jose, California

(*Received* 26 *July* 1957)

SUMMARY

The flow past a flat plate at Reynolds numbers in the range 0·1 to 10·0 is investigated by an analogue method. The solution gives the stream function and the vorticity in the flow field surrounding the plate. From these are obtained the local coefficient of friction, the pressure distribution along the plate, and the total drag coefficient. The drag coefficient approaches the analytical values of Haaser (1950) and of Tomotika & Aoi (1953) as the Reynolds number decreases toward 0·1. The drag coefficient approaches the Blasius solution as the Reynolds number increases. At Reynolds number 10·0 the drag coefficient is still above the Blasius value, but is below the value obtained experimentally by Janour (1951). The difference from the experimental result is attributed for the most part to truncation error.

INTRODUCTION

The Blasius solution of the Prandtl boundary layer equation, for the case of flow past a thin flat plate, is valid only for a boundary layer whose thickness is very small relative to distance from the leading edge. The results of the Blasius analysis are therefore invalid at low Reynolds numbers. Kuo (1953) has investigated the flow past a flat plate for Reynolds numbers as low as 10 by a perturbation method. Tomotika & Aoi (1953), Imai (1954), and others have investigated the flow past a flat plate for Reynolds numbers up to about 1·0, by linearizing the flow equation in accordance with the Oseen approximation. Haaser (1950) has computed the skin friction distribution for this configuration, using Carrier's (1953) modification of the Oseen linearization for Reynolds numbers up to 5·0. The object of this paper is to investigate, by an analogue method, the flow past a finite flat plate at Reynolds numbers in the range 0·1 to 10·0, using the exact non-linear formulation of the problem, and to compare the results with those of the foregoing and with experiment.

The equation governing the two-dimensional motion of an incompressible fluid with constant viscosity is

$$\mathbf{v}.\nabla\zeta = \nu\nabla^2\zeta \tag{1}$$

where ζ is the scalar vorticity, given by

$$\zeta = \frac{\partial v}{\partial \psi} - \frac{\partial u}{\partial y}. \tag{2}$$

The defining equations of a stream function ψ are

$$u = -\frac{\partial \psi}{\partial y}, \qquad v = \frac{\partial \psi}{\partial x}. \tag{3}$$

In Cartesian coordinates, these equations may be written

$$\nabla^2 \zeta = \frac{1}{\nu}\left\{\frac{\partial \psi}{\partial x}\frac{\partial \zeta}{\partial y} - \frac{\partial \psi}{\partial y}\frac{\partial \zeta}{\partial x}\right\}, \tag{4}$$

$$\nabla^2 \psi = \zeta. \tag{5}$$

Equations (3) satisfy the continuity equation which, therefore, does not need to be expressed explicitly.

Equations (4) and (5) have the form of the Poisson equation. These particular equations have been solved for the case of flow past a circular cylinder with zero circulation at Reynolds numbers in the range 1 to 1000, by numerical techniques (Thom 1933; Kawaguti 1953; and Allen & Southwell 1955). The procedure outlined in this paper gives a method of solution by means of two resistance networks which is applicable to an extensive class of problems in viscous flow. It will be applied here specifically to the case of flow past a flat plate.

Transformation of equations

It is convenient at the outset to render the equation dimensionless, and to consider transformation from the physical plane to some other plane. Let the physical plane be the z-plane, and let the velocity of the undisturbed flow be parallel to the x-axis. Then

$$z' = x' + iy' = r' e^{i\theta}.$$

Here the prime notation signifies dimensional quantities. The hydrodynamic equations, as well as the expression for z, are rendered dimensionless by making the following substitutions:

$$z = \frac{z'}{r_0'}, \qquad u = \frac{u'}{u_\infty'}, \qquad v = \frac{v'}{u_\infty'}, \qquad p = \frac{p'}{\rho'(u_\infty')^2},$$

$$\nu = \frac{\nu'}{u_\infty' r_0'}, \qquad \psi = \frac{\psi'}{u_\infty' r_0'}, \qquad \zeta = \frac{\zeta' r_0'}{u_\infty'}, \qquad N_R = \frac{2u_\infty' r_0'}{\nu'},$$

where r_0' is some characteristic length, e.g. a cylinder radius, u_∞' is the undisturbed velocity parallel to the x-axis, ν' is the kinematic viscosity and N_R is the Reynolds number.

The transformation $t = f(z)$ can be employed to map the field on to the t-plane where

$$t = \xi + i\eta. \tag{6}$$

If the transformation is conformal, equations (4) and (5) become

$$\nabla_t^2 \zeta = \frac{N_R}{2}\left\{\frac{\partial \psi}{\partial \xi}\frac{\partial \zeta}{\partial \eta} - \frac{\partial \psi}{\partial \eta}\frac{\partial \zeta}{\partial \xi}\right\} \tag{7}$$

and

$$\nabla_t^2 \psi = \frac{1}{q^2}\zeta, \tag{8}$$

where
$$\nabla_t^2 = \frac{\partial^2}{\partial \xi^2} + \frac{\partial^2}{\partial \eta^2}$$

and q, the transformation modulus, is the ratio of a length in the t-plane to the corresponding length in the z-plane, and is a function of position, that is
$$q = \left|\frac{dt}{dz}\right| = q(x,y) = q(\xi,\eta).$$

Solution of the Poisson equation by a network analogue

The general form of the Poisson equation
$$\nabla^2\phi = f(x,y) \tag{9}$$
may be expressed approximately in the difference form
$$\phi_0 = \phi_M - \tfrac{1}{4}a^2 f(x_0,y_0), \tag{10}$$
where the field has been divided into square meshes of length a on a side (figure 1). ϕ_0 is the value of the function in question at a particular mesh point, and ϕ_M is the average for the nearest four neighbouring mesh points.

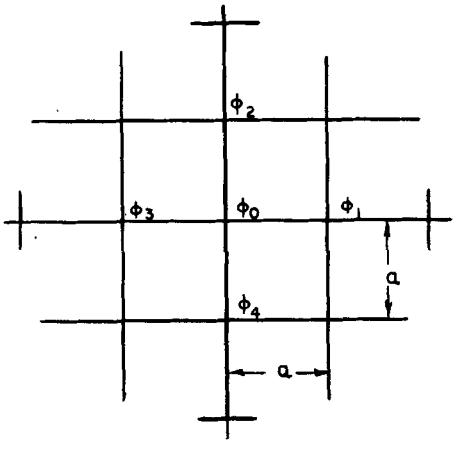

Figure 1. Representation of field by a net.

Now consider a resistance network having a geometrically similar mesh pattern (figure 2), with resistances R_j between adjacent mesh points (nodes) as shown. In addition to the current flowing through these resistors, current flows into each of the nodes from an external source. The sum of the currents flowing into a particular node must be zero from Kirchhoff's law of node currents:
$$\frac{e_0-e_1}{R_1} + \frac{e_0-e_2}{R_2} + \frac{e_0-e_3}{R_3} + \frac{e_0-e_4}{R_4} - i_0 = 0,$$
$$\delta R_j = R_j - R_1,$$
$$e_0 = e_M - \left[\frac{1}{4}\sum_{j=2}^{4}\frac{\delta R_j}{R_j}e_j - \frac{e_0}{4}\sum_{j=2}^{4}\frac{\delta R_j}{R_j} - \frac{R_1 i_0}{4}\right], \tag{11}$$

where δR_j is the deviation of the jth resistor with respect to the first resistor. The analogy that exists between the function ϕ of the system described by equation (10) and the voltage e of the network is apparent. If a scale factor K is chosen so that $e = K\phi$ at corresponding points, then i can be adjusted so that

$$i_0 = \frac{1}{R_1}\sum_{j=2}^{4}\frac{\delta R_j}{R_j}e_j - \frac{e_0}{R_1}\sum_{j=2}^{4}\frac{\delta R_j}{R_j} - \frac{Ka^2}{R_1}f(x_0, y_0). \tag{12}$$

Note that when the resistor deviation is zero the first two terms on the right of equation (12), which are in fact error terms due to this deviation, drop out. By the method of this paper, however, it is not necessary that the resistor deviation be zero, as the current i_0 itself is not measured, and the network resistor deviation contributes nothing to the computational error.

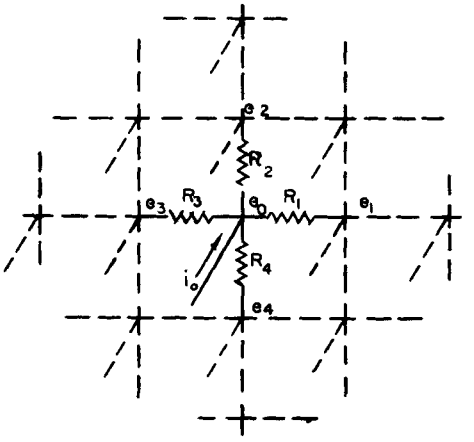

Figure 2. Resistance network pattern geometrically similar to net of figure 1.

The Poisson equations whose solutions are desired are equations (7) and (8). The difference forms of these equations are, respectively,

$$\zeta_0 = \zeta_M - \tfrac{1}{32}N_R\{(\psi_1-\psi_3)(\zeta_2-\zeta_4)-(\psi_2-\psi_4)(\zeta_1-\zeta_3)\} \tag{13}$$

and

$$\psi_0 = \psi_M - \frac{a^2}{4q_0}\zeta_0, \tag{14}$$

where

$$\zeta_M = \tfrac{1}{4}(\zeta_1+\zeta_2+\zeta_3+\zeta_4), \qquad \psi_M = \tfrac{1}{4}(\psi_1+\psi_2+\psi_3+\psi_4).$$

There is a network for each equation. The voltages at the boundaries of the two networks are fixed to correspond to the boundary conditions of the problem. Current must then be supplied to each anode in the ψ-network proportional (except for the resistor deviation terms of (12)) to ζ for that point, and to each node in the ζ-network proportional to $\{(\psi_1-\psi_3)(\zeta_2-\zeta_4)-(\psi_2-\psi_4)(\zeta_1-\zeta_3)\}$ for that point. To accomplish this quantities, called the 'residuals' in relaxation procedures, are defined by

$$\mathscr{R}_\psi = 4\psi_M - 4\psi_0 - \frac{a^2}{q^2}\zeta_0 \tag{15}$$

for the ψ-net, and by

$$\mathscr{R}_\zeta = 4\zeta_M - 4\zeta_0 - \tfrac{1}{8}N_R\{(\psi_1-\psi_3)(\zeta_2-\zeta_4)-(\psi_2-\psi_4)(\zeta_1-\zeta_3)\} \qquad (16)$$

for the ζ-net. The current to each node in the ψ-network is adjusted manually until $\mathscr{R}_\psi$ goes to zero, and the current to each node in the ζ-network is adjusted manually until $\mathscr{R}_\zeta$ goes to zero. $\mathscr{R}_\psi$ and $\mathscr{R}_\zeta$ may be computed electronically by using components which change sign, add or multiply (the theory is clearly presented in a number of texts, for example see Korn & Korn (1952) or Soroka (1954)). A schematic diagram of the networks and associated voltage sources, current controls, etc., is shown in figure 3. One arrangement of electronic components for computing residuals is shown schematically in figure 4.

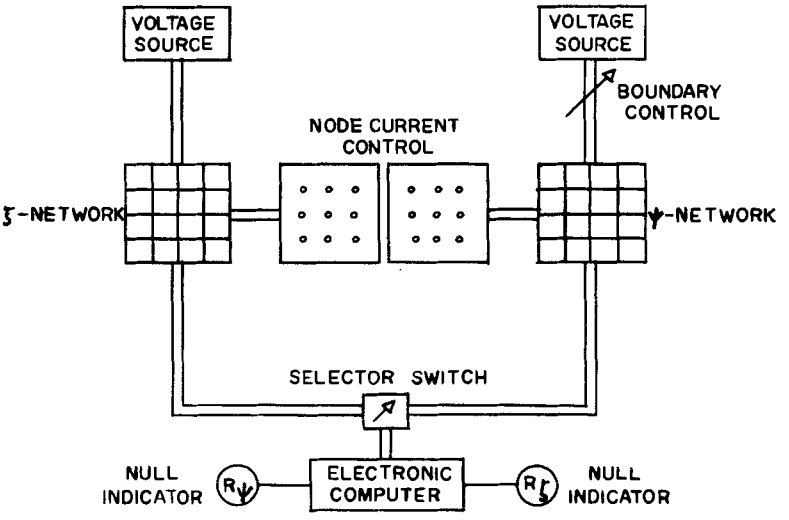

Figure 3. Schematic diagram of analogue.

The solution to equations (13) and (14) is obtained after a relaxation procedure involving the adjustment of the currents to each of the nodes in the two networks in several successive steps. This is the approximate solution to equations (7) and (8), the degree of approximation improving with the fineness of mesh. A mesh size should be used such that any decrease in the size will produce no change in the solution within the desired limits of accuracy.

Boundary conditions (general)

In the case of a flat plate located at or near the origin in an otherwise uniform flow field, ψ is essentially at its uniform field value, and ζ is zero, far away from the origin. Thus, this part of the boundary, henceforth referred to as the outer boundary, is chosen far away and this may be taken care of by making the network quite large. It may also be handled by using a transformation which permits a reasonably small network to be used as was done in obtaining the results reported in this paper.

ψ will be known at every place on the boundary and ζ will be known at every place except where the boundary is solid (that is, along the flat plate). Consider a solid boundary which is parallel to the ξ-axis (figure 5). The

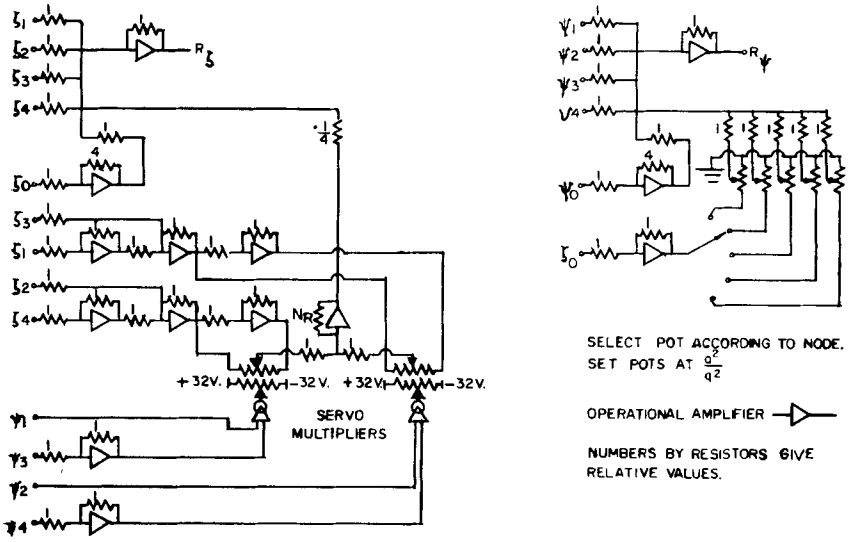

Figure 4. Assembly of electronic components for computing residuals.

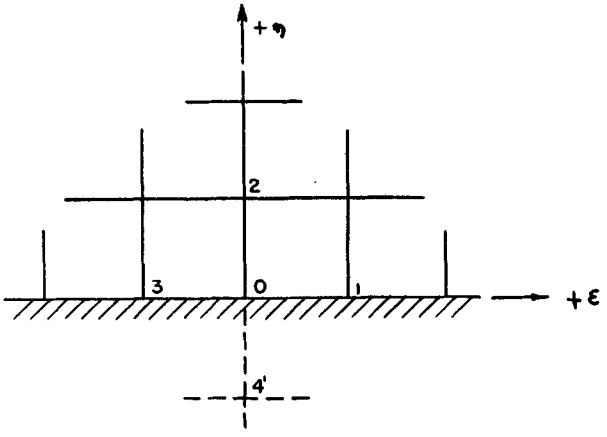

Figure 5. Solid boundary parallel to ξ-axis.

value of ζ at the point 0 on the boundary is desired. Points 1 and 3 are on the boundary and point 2 is a short distance inside the boundary at a position on a normal through point 0. The expression for ζ in terms of ψ follows from equation (8):

$$\zeta = q_0^2[\nabla_i^2 \psi]_0 = q_0^2\left[\left(\frac{\partial^2\psi}{\partial\xi^2}\right)_0 + \left(\frac{\partial^2\psi}{\partial\eta^2}\right)_0\right]. \tag{17}$$

A difference form for equation (17) may be obtained by using a Taylor

series expansion about point 0. The expression for the stream function at point 2 is

$$\psi_2 = \psi_0 + a\left(\frac{\partial\psi}{\partial\eta}\right)_0 + \frac{a^2}{2}\left(\frac{\partial^2\psi}{\partial\eta^2}\right)_0 + \frac{a^3}{6}\left(\frac{\partial^3\psi}{\partial\eta^3}\right)_0 + \frac{a^4}{24}\left(\frac{\partial^4\psi}{\partial\eta^4}\right)_0 + o(a^5).$$

From equation (8),

$$\left(\frac{\partial^2\psi}{\partial\eta^2}\right)_0 = -\left(\frac{\partial^2\psi}{\partial\xi^2}\right)_0 + \frac{1}{q_0^2}\zeta_0,$$

$$\left(\frac{\partial^3\psi}{\partial\eta^3}\right)_0 = -\left[\frac{\partial^2}{\partial\xi^2}\left(\frac{\partial\psi}{\partial\eta}\right)\right]_0 + \left(\frac{\partial(\zeta/q^2)}{\partial\eta}\right)_0,$$

$$\left(\frac{\partial^4\psi}{\partial\eta^4}\right)_0 = \left(\frac{\partial^4\psi}{\partial\xi^4}\right)_0 + \left(\frac{\partial^2(\zeta/q^2)}{\partial\eta^2}\right)_0 - \left(\frac{\partial^2(\zeta/q^2)}{\partial\xi^2}\right)_0.$$

Along the solid boundary ψ is constant and u is zero. Hence, all derivatives of ψ with respect to ξ, and the first derivative of ψ with respect to η, are zero. ψ_2 is now given by

$$\psi_2 = \psi_0 + \frac{a^2}{2}\frac{\zeta_0}{q_0^2} + \frac{a^3}{6}\left(\frac{\partial(\zeta/q^2)}{\partial\eta}\right)_0 + \frac{a^4}{24}\left[\left(\frac{\partial^2(\zeta/q^2)}{\partial\eta^2}\right)_0 - \left(\frac{\partial^2(\zeta/q^2)}{\partial\xi^2}\right)_0\right]. \quad (18)$$

Neglecting all terms past the second on the right (that is, all terms of order a^3 or higher), and rearranging, one obtains

$$\zeta_0 = \frac{2q_0^2}{a^2}(\psi_2 - \psi_0). \quad (19)$$

Thom (1933) and Allen & Southwell (1955) have used equation (19), and their results check well with experiment. It was possible for them to decrease the mesh constant a in regions where $(\partial\zeta/\partial n)_s$ was large, thus keeping the third (and following) term on the right of equation (18) small and presumably negligible. Woods (1954), on the other hand, takes the third term into account in the following manner. The Taylor series is again employed, this time to obtain an expression for the vorticity at point 2:

$$\frac{\zeta_2}{q_2^2} = \frac{\zeta_0}{q_0^2} + a\left(\frac{\partial(\zeta/q^2)}{\partial\eta}\right)_0 + \frac{a^2}{2}\left(\frac{\partial^2(\zeta/q^2)}{\partial\eta^2}\right)_0 + o(a^3).$$

Rearrangement and multiplication by $\frac{1}{6}a^2$ gives

$$\frac{a^3}{6}\left(\frac{\partial(\zeta/q^2)}{\partial\eta}\right)_0 = \frac{a^2}{6}\frac{\zeta_2}{q_2^2} - \frac{a^2}{6}\frac{\zeta_0}{q_0^2} - \frac{a^4}{12}\left(\frac{\partial^2(\zeta/q^2)}{\partial\eta^2}\right)_0 + o(a^5),$$

and substitution for the third term in (18) then gives

$$\psi_2 = \psi_0 + \frac{a^2}{3}\frac{\zeta_0}{q_0^2} + \frac{a^2}{6}\frac{\zeta_0}{q_2^2} - \frac{a^4}{24}\left[\nabla_t^2\frac{\zeta}{q^2}\right]_0 + o(a^5). \quad (20)$$

Neglect of all terms in (20) of order a^4 or higher, and rearrangement, finally gives

$$\zeta_0 = \frac{3q_0^2}{a^2}(\psi_2 - \psi_0) - \frac{q_0^2}{2q_2^2}\zeta_2, \quad (21\,a)$$

or, more generally,

$$\zeta_s = \frac{3q_s^2}{m^2}(\psi_p - \psi_s) - \frac{q_s^2}{2q_p^2}\zeta_p, \tag{21 b}$$

where ζ_s is the vorticity at any point s on the solid boundary, ψ_s is the stream function at that point, ζ_p is the vorticity at a point p inside the boundary at a distance m on a normal through s, and ψ_p is the stream function at point p.

Equation (21) is preferable to (19) for use with networks unless the mesh constant has been reduced in regions of the flow field where the vorticity gradient is steep. Equation (21) was used in obtaining the results reported in this paper.

Values of ζ_s for every point on the solid boundary are first assumed, then new values are determined after each relaxation of the two networks. If succeeding values of ζ_s are based on equation (21 b), that is,

$$\zeta_s^{(n+1)} = \frac{3q_s^2}{m^2}(\psi_p^{(n)} - \psi_s) - \frac{q_s^2}{2q_p^2}\zeta_p^{(n)},$$

where the superscript in parentheses refers to the number of the step in the iteration, the process will diverge. To effect convergence a plot of $\{\zeta_s + (q_s^2/2q_p^2)\zeta_p\}^{(n)}$ *vs* $\psi_p^{(n)}$ may be prepared and the graph of equation (21 b) superposed. The intersection of the two curves will give the final value of $\{\zeta_s + (q_s^2/2q_p^2)\zeta_p\}$. A supplementary plot of $\zeta_s^{(n)}$ *vs* $\{\zeta_s + (q_s^2/2q_p^2)\zeta_p\}^{(n)}$ may assist in estimating the correct final value of ζ_s.

Flow past a flat plate

Consider the case of a finite flat plate (of infinitesimal thickness) in an infinite flow field, and parallel to the otherwise undisturbed velocity, with leading edge at $(-1, 0)$ and trailing edge at $(+1, 0)$. Let the transformation be

$$z = \cosh t, \tag{22}$$

for which the modulus is

$$q = [\sinh^2\xi + \sin^2\eta]^{-1/2}. \tag{23}$$

This transformation has the following features:

(1) the modulus is very small far away from the origin, thus permitting the transformation plane to be relatively small;

(2) the modulus is very large in the region of the leading edge, thus literally magnifying the region of interest.

Because the flow will be symmetrical only the half plane need be used. The transformation is illustrated in figure 6.

The boundary conditions are:

$$\xi = 0, \qquad \psi = 0, \qquad \frac{\partial\psi}{\partial\xi} = 0;$$

$$\xi = \xi_\infty, \qquad \psi = -\sinh\xi_\infty \sin\eta, \qquad \zeta = 0;$$

$$\eta = 0,\ \pi, \qquad \psi = 0, \qquad \zeta = 0.$$

The solution obtained from the analogue represents ψ and ζ as functions of position in the flow field (including the solid boundary). The velocity is given by (3). The equation for the pressure is

$$\frac{p-p_\infty}{\frac{1}{2}u_\infty^2} = 1+2\int_\infty \left(\zeta\frac{\partial\psi}{\partial\xi} - \frac{2}{N_R}\frac{\partial\zeta}{\partial\eta}\right)d\xi + 2\int_\infty \left(\zeta\frac{\partial\psi}{\partial\eta} + \frac{2}{N_R}\frac{\partial\zeta}{\partial\xi}\right)d\eta. \quad (24)$$

The shear stress is given by

$$\tau_s = -\frac{2}{N_R}\zeta_s. \quad (25)$$

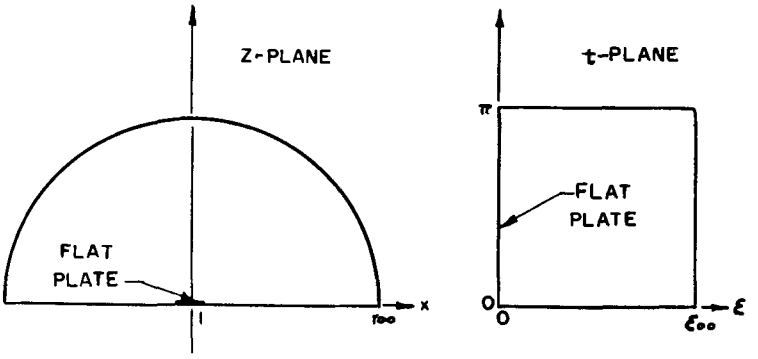

Figure 6. Transformation for a flat plate.

The local coefficient of friction c_f is equal numerically to twice the dimensionless shear stress of equation (25). Let the defining equation for the drag coefficient C_D be

$$D' = C_D \tfrac{1}{2}l'\rho' u_\infty'^2,$$

where D' is the drag on both sides of the plate per unit span, and l' is the dimension of the plate parallel to the flow. Then C_D is given by

$$C_D = \frac{1}{2}\int_{-1}^{+1} c_f\,dx = -\frac{1}{2}\int_\pi^0 c_f \sin\eta\,d\eta. \quad (26)$$

Results and discussion

Two networks were constructed, with outer boundary at $\xi_\infty = \frac{5}{4}\pi$* and with mesh constant equal to $\frac{1}{8}\pi$† (a transition to $\frac{1}{4}\pi$ was effected beyond $\xi = \frac{1}{4}\pi$). The REAC of the Rand Corporation, Santa Monica, California, was made available to the author for the purpose of computing residuals, its components being connected as indicated in figure 4. Data obtained from the analogue in the form of potentials were readily converted to stream function and vorticity by the application of the appropriate scale factors.

* Location of the outer boundary was based on a consideration of the distance from the plate at which the maximum vorticity in a laminar wake would have become small enough to neglect.

† Considerations based on limiting the truncation error in ζ led to the value $\frac{1}{40}\pi$ for the mesh constant. This was increased by a factor of 5 for reasons of economy. Any error present in the solution is presumed to be largely truncation error.

Solutions were obtained for Reynolds numbers 0·1, 1·0, and 10·0. The corresponding values of ψ and ζ are given in tables 1 and 2. The differentation and integration involved in determining the pressure and drag coefficient were done numerically.

The local coefficient of friction is plotted *vs* x, for the three Reynolds numbers, in figure 7. c_f as given by the Blasius solution is also plotted. The analogue solution approaches the Blasius solution as the Reynolds number increases. The influence of the trailing edge, significant at very low Reynolds numbers, may be seen distinctly in the analogue solution. The Blasius solution, of course, does not take the effect of the trailing edge into account.

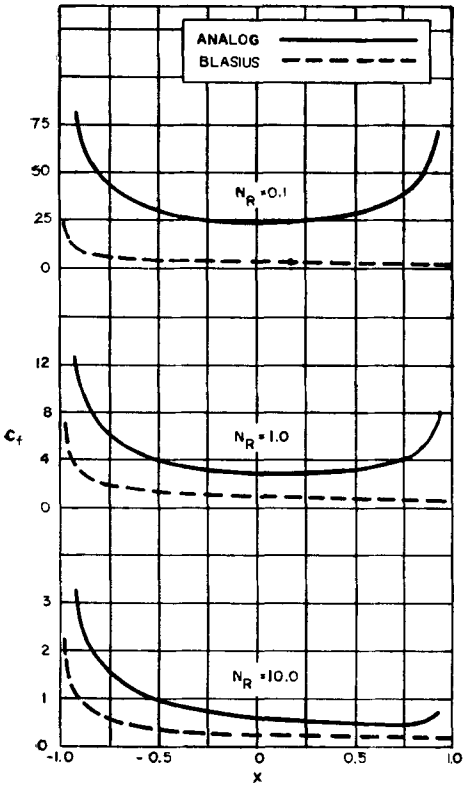

Figure 7. Local friction coefficient *vs* x.

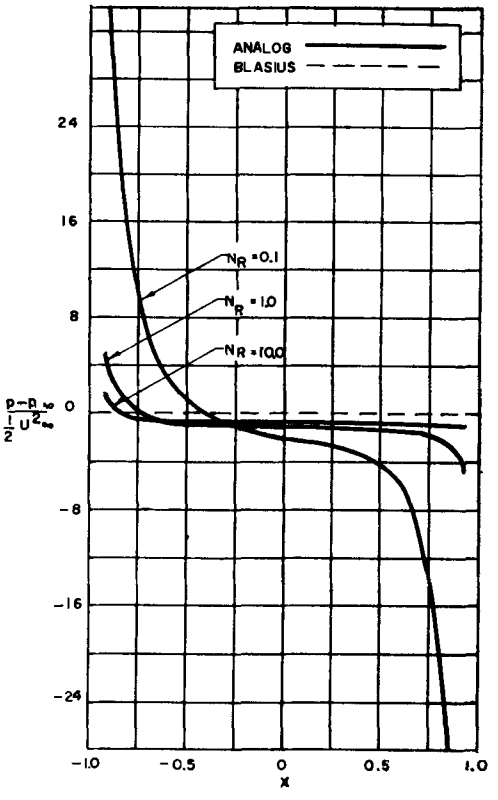

Figure 8. Pressure *vs* x.

The pressure at the surface of the plate was found by first integrating the terms of (24) from the outer boundary to the plate along the path $\eta = \frac{1}{2}\pi$ (and thereby determining the pressure at the mid-point of the plate), and then integrating along the surface of the plate (that is, along the path $\xi = 0$). The pressure is plotted *vs* x, for the three Reynolds numbers, in figure 8. The value given by the Blasius solution is zero everywhere. It may again be noted that the analogue solution approaches the Blasius solution as the Reynolds number increases.

The drag coefficient C_D is given by (26). One should know c_f at every point along the x-axis from $x = -1$ to $x = +1$ in order to evaluate the integral. But the analogue gives values only from $x = -0{\cdot}924$ to $x = +0{\cdot}924$. The fact that c_f is not known in the regions adjacent to the leading and trailing edges is a serious deficiency. However, some correlation is established between the solutions at the three Reynolds numbers by plotting c_f *vs* the 'local' Reynolds numbers N_{Rx} and $N_{R(l-x)}$ in

η	N_R	$\xi = 0$	$\frac{1}{8}\pi$	$\frac{1}{4}\pi$	$\frac{3}{8}\pi$	$\frac{1}{2}\pi$	$\frac{3}{4}\pi$	π	$\frac{5}{4}\pi$
$\frac{7}{8}\pi$	0·1	0	−0·022	−0·08	−0·21	—	—	—	—
	1·0	0	−0·030	−0·11	−0·28	—	—	—	—
	10·0	0	−0·076	−0·27	−0·57	—	—	—	—
$\frac{3}{4}\pi$	—	0	−0·038	−0·15	−0·38	−0·79	−2·57	−7·18	−17·94
	—	0	−0·050	−0·20	−0·50	−1·04	−3·21	−8·04	−17·94
	—	0	−0·120	−0·46	−1·00	−1·72	−3·89	−8·42	−17·94
$\frac{5}{8}\pi$	—	0	−0·047	−0·19	−0·48	—	—	—	—
	—	0	−0·060	−0·25	−0·61	—	—	—	—
	—	0	−0·131	−0·54	−1·21	—	—	—	—
$\frac{1}{2}\pi$	—	0	−0·049	−0·20	−0·51	−1·07	−3·48	− 9·86	−25·36
	—	0	−0·060	−0·25	−0·62	−1·30	−4·14	−11·10	−25·37
	—	0	−0·116	−0·49	−1·16	−2·20	−5·39	−11·89	−25·37
$\frac{3}{8}\pi$	—	0	−0·045	−0·18	−0·46	—	—	—	—
	—	0	−0·051	−0·20	−0·51	—	—	—	—
	—	0	−0·079	−0·33	−0·81	—	—	—	—
$\frac{1}{4}\pi$	—	0	−0·035	−0·14	−0·34	−0·71	−2·31	−6·63	−17·94
	—	0	−0·036	−0·14	−0·35	−0·70	−2·20	−6·27	−17·94
	—	0	−0·042	−0·17	−0·41	−0·79	−3·64	−8·38	−17·94
$\frac{1}{8}\pi$	—	0	−0·020	−0·07	−0·19	—	—	—	—
	—	0	−0·021	−0·07	−0·18	—	—	—	—
	—	0	−0·018	−0·06	−0·14	—	—	—	—

Table 1. Stream function.

figures 9 and 10 respectively. N_{Rx} is the local Reynolds number based on distance from the leading edge and $N_{R(l-x)}$ is the local number based on distance from the trailing edge. On the basis of these plots a straight line extrapolation (on logarithmic coordinates) is employed to obtain values of c_f in the regions $-1 < x < -0{\cdot}924$ and $+0{\cdot}924 < x < +1$, the slope of the straight line being taken as $-0{\cdot}577$.

C_D is now given by

$$C_D = \frac{1}{2}\int_{-1}^{-0{\cdot}924} c_f\,dx - \frac{1}{2}\int_{\frac{1}{8}\pi}^{\frac{7}{8}\pi} c_f \sin\eta\,d\eta + \frac{1}{2}\int_{0{\cdot}924}^{1} c_f\,dx.$$

The first term on the right is the contribution of the 3·8% segment of the surface adjacent to the leading edge, the last term is the contribution of the 3·8% segment adjacent to the trailing edge, and the middle term is the contribution of the 92·4% of the surface which lies between. Let these

η	N_R	$\xi = 0$	$\frac{1}{8}\pi$	$\frac{1}{4}\pi$	$\frac{3}{8}\pi$	$\frac{1}{2}\pi$	$\frac{3}{4}\pi$	π	$\frac{5}{4}\pi$
$\frac{7}{8}\pi$	0·1	−1·99	−0·76	−0·34	−0·15	—	—	—	—
	1·0	−2·92	−1·07	−0·44	−0·16	—	—	—	—
	10·0	−7·75	−2·05	−0·21	+0·11	—	—	—	—
$\frac{3}{4}\pi$	—	−0·97	−0·69	−0·44	−0·27	−0·18	−0·07	−0·02	0
	—	−1·38	−0·95	−0·56	−0·31	−0·16	−0·02	0	—
	—	−3·68	−1·94	−0·40	+0·06	0	—	—	—
$\frac{5}{8}\pi$	—	−0·70	−0·60	−0·45	−0·32	—	—	—	—
	—	−0·89	−0·77	−0·56	−0·37	—	—	—	—
	—	−2·21	−1·62	−0·58	−0·04		—	—	—
$\frac{1}{2}\pi$	—	−0·61	−0·56	−0·45	−0·33	−0·23	−0·11	−0·04	0
	—	−0·74	−0·68	−0·54	−0·39	−0·25	−0·07	+0·01	0
	—	−1·53	−1·34	−0·72	−0·17	0	—	—	—
$\frac{3}{8}\pi$	—	−0·66	−0·58	−0·44	−0·32	—	—	—	—
	—	−0·75	−0·67	−0·52	−0·39	—	—	—	—
	—	−1·31	−1·17	−0·84	−0·46	—	—	—	—
$\frac{1}{4}\pi$	—	−0·90	−0·65	−0·42	−0·27	−0·19	−0·09	−0·04	0
	—	−0·94	−0·72	−0·49	−0·34	−0·25	−0·14	−0·08	0
	—	−1·20	−1·05	−0·85	−0·66	−0·80	0	—	—
$\frac{1}{8}\pi$	—	−1·82	−0·70	−0·32	−0·16	—	—	—	—
	—	−2·01	−0·78	−0·37	−0·20	—	—	—	—
	—	−1·84	−0·91	−0·64	−0·58	—	—	—	—

Table 2. Vorticity.

N_R	C_{D1}	C_{D2}	C_{D3}	C_D
0·1	7·09	30·6	6·76	44·45
1·0	1·07	3·78	0·75	5·60
10·0	0·28	0·79	0·07	1·14

Table 3. Drag coefficient.

contributions to C_D be denoted respectively by C_{D1}, C_{D3}, and C_{D2}, so that $C_D = C_{D1} + C_{D2} + C_{D3}$. The drag coefficient, together with its three parts, is given in table 3.

According to this analysis the contribution of the leading edge segment increases from 16% to 25% of the total drag, the contribution of the trailing

edge segment decreases from 15% to 6%, and the contribution of the surface between stays nearly constant at 68% or 69% as the Reynolds number is increased from 0·1 to 10·0. This is in contrast to the Blasius

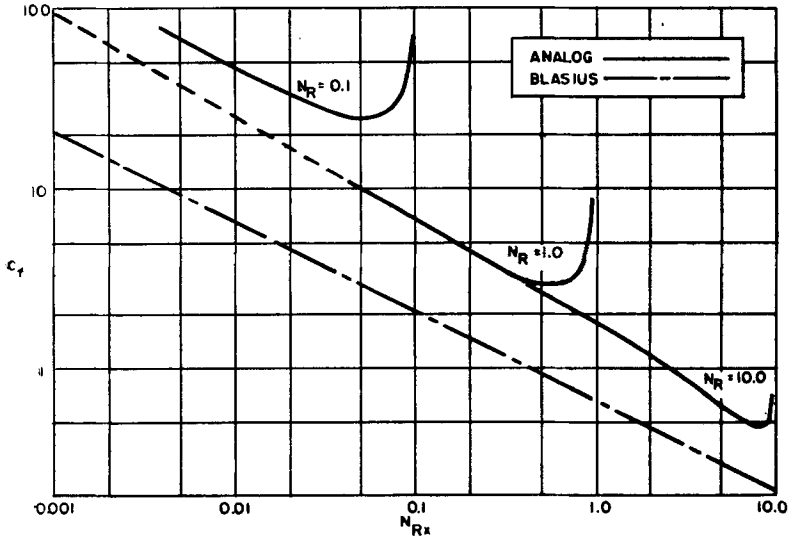

Figure 9. Local coefficient of friction *vs* N_{rx}.

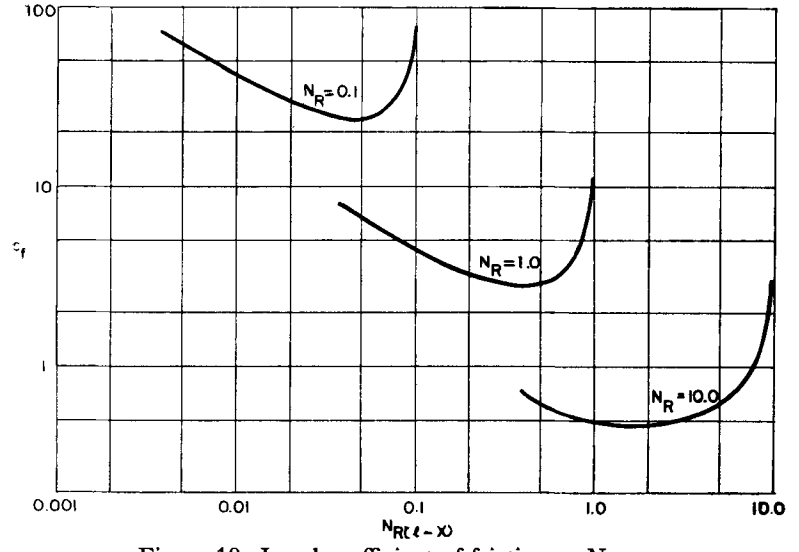

Figure 10. Local coefficient of friction *vs* $N_{R(l-x)}$.

solution according to which the contribution of the same leading edge segment is constant at 13·75% of the total drag and the contribution of the trailing edge segment is constant at 1·35% of the total drag, for all Reynolds numbers.

The drag data of table 3 are compared with the experimental values reported by Janour (1951) in figure 11. Drag data reported by Sherman (1952) are also shown although these were obtained under compressible flow conditions at Mach numbers of approximately 0·2 and 0·6. Also shown are the drag coefficient for the Blasius solution and the drag coefficients as determined by Tomotika & Aoi (1953) and Haaser (1950), the latter two being based respectively on the Oseen approximation and on Carrier's (1953) modification of the Oseen approximation. The drag coefficient as

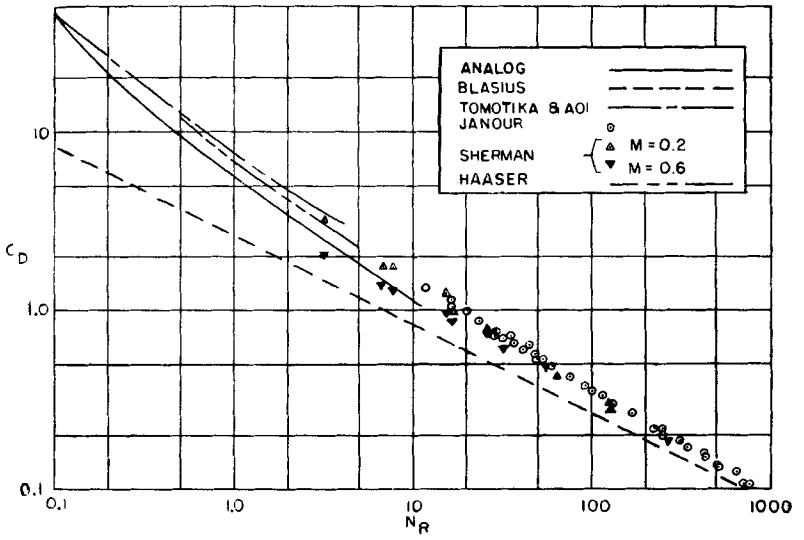

Figure 11. Drag coefficient *vs* Reynolds number.

determined from the analogue solution approaches the Blasius solution as the Reynolds number increases, and approaches the solutions of Haaser and of Tomotika & Aoi as the Reynolds number decreases. In the range where comparison with experiment is possible, the drag coefficient lies below the values of Janour and Sherman. This difference from experiment is believed to be due chiefly to truncation error.

The author wishes to thank the Rand Corporation, Santa Monica, California, for making available to him their analogue computing facilities. The solutions reported here were all obtained at Rand. The resistance networks and associated switching equipment were made possible by the University of California Research Grant No. 1115.

References

Allen, D. N. & Southwell, R. V. 1955 Relaxation methods applied to determine the motion, in two dimensions, of a viscous fluid past a fixed cylinder, *Quart. J. Mech. Appl. Math.* **8**, 129.

Carrier, G. F. 1953 On slow viscous flow, final report, Office of Naval Research Contract Nonr–653 (00).

HAASER, N. B. 1950 The viscous flow past a flat plate, Ph.D. Thesis, Graduate Division of Applied Mathematics, Brown University.

IMAI, I. 1954 A method of solving Oseen's equations and its application to the flow past an inclined elliptic cylinder, *Proc. Roy. Soc.* A, **224,** 141.

JANOUR, Z. 1951 Resistance of a plate in parallel flow at low Reynolds numbers, *Nat. Adv. Comm. Aero., Wash., Tech. Mem.* no. 1316.

KAWAGUTI, M. 1953 Numerical solution of the Navier–Stokes equations for the flow around a circular cylinder at Reynolds number 40, *J. Phys. Soc. Japan* **8,** 747.

KORN, G. A. & KORN, T. M. 1952 *Electronic Analog Computers.* New York · McGraw-Hill.

KUO, Y. H. 1953 On the flow of an incompressible viscous fluid past a flat plate at moderate Reynolds number, *J. Math. Phys.* **32,** 83.

SHERMAN, F. S. 1952 Skin friction in subsonic low density gas flow, *University of California, IER Report* no. HE–150–105.

SOROKA, W. W. 1954 *Analog Methods in Computation and Simulation.* New York : McGraw-Hill.

THOM, A. 1933 The flow past circular cylinders at low speeds, *Proc. Roy. Soc.* A, **141,** 651.

TOMOTIKA, S. & AOI, T. 1953 The steady flow of a viscous fluid past an elliptic cylinder and a flat plate at small Reynolds numbers, *Quart. J. Mech. Appl. Math.* **6,** 290.

WOODS, L. C. 1954 A note on the numerical solution of fourth order differential equations, *Aero. Quart.* **5,** 176.